

# THE REIONIZATION HISTORY AT HIGH REDSHIFTS I: PHYSICAL MODELS AND NEW CONSTRAINTS FROM CMB POLARIZATION

ZOLTÁN HAIMAN

Department of Astronomy, Columbia University, 550 West 120th Street, New York, NY 10027

GILBERT P. HOLDER

Institute for Advanced Study, School of Natural Sciences, Olden Lane, Princeton, NJ 08540

*Submitted to ApJ*

## ABSTRACT

The recent discovery of a high optical depth  $\tau$  to Thomson scattering from the Wilkinson Microwave Anisotropy Probe (*WMAP*) data implies that significant reionization took place at redshifts  $z > 6$ . This discovery has important implications for the sources of reionization, and allows, for the first time, constraints to be placed on physical reionization scenarios out to redshift  $z \sim 20$ . Using a new suite of semi-analytic reionization models, we show that the high value of  $\tau$  requires a surprisingly high efficiency  $\epsilon$  of the first generation of UV sources for injecting ionizing photons into the intergalactic medium. We find that no simple reionization model can be consistent with the combination of the *WMAP* result with data from the  $z \lesssim 6.5$  universe. Satisfying both constraints requires either of the following: (i)  $\text{H}_2$  molecules form efficiently at  $z \sim 20$ , survive feedback processes, and allow UV sources in halos with virial temperatures  $T_{\text{vir}} < 10^4 \text{K}$  to contribute substantially to reionization, or (ii) the efficiency  $\epsilon$  in halos with  $T_{\text{vir}} > 10^4 \text{K}$  decreased by a factor of  $\gtrsim 30$  between  $z \sim 20$  and  $z \sim 6$ . We discuss the relevant physical issues to produce either scenario, and argue that both options are viable, and allowed by current data. In detailed models of the reionization history, we find that the evolution of the ionized fractions in the two scenarios have distinctive features that Planck can distinguish at  $\gtrsim 3\sigma$  significance. At the high *WMAP* value for  $\tau$ , Planck will also be able to provide tight statistical constraints on reionization model parameters, and elucidate much of the physics at the end of the Dark Ages. The sources responsible for the high optical depth discovered by *WMAP* should be directly detectable out to  $z \sim 15$  by the *James Webb Space Telescope*.

## 1. INTRODUCTION

How and when the intergalactic medium (IGM) was reionized is one of the long outstanding questions in astrophysical cosmology, holding many clues about the onset of structure formation in cold dark matter (CDM) cosmologies, and the nature of the first generation of light sources. The past year has seen an explosion of progress in probing the reionization history, culminating in recent results from the *WMAP* satellite (Bennett et al. 2003). Spectroscopic observations of high redshift quasars had previously found no strong HI absorption (a so-called ‘‘Gunn–Peterson’’, GP trough) in sources at  $z \lesssim 6$ , showing that the IGM is highly ionized at these redshifts (Fan et al. 2000). However, the discoveries of a handful of bright quasars in the Sloan Digital Sky Survey (SDSS) at redshifts  $z > 6$  have revealed full GP troughs, i.e. spectra consistent with no flux at high S/N over a substantial stretch of wavelength shortward of  $(1+z)\lambda_\alpha = 8850 \text{\AA}$  (Becker et al. 2001; Fan et al. 2003). The lack of any detectable flux translates to strong lower limits  $x_{\text{H}} \gtrsim 0.01$  on the mean mass-weighted neutral fraction of the IGM at  $z \sim 6$  (Cen & McDonald 2002; Fan et al. 2002; Lidz et al. 2002; Pentericci et al. 2002). Comparisons with numerical simulations of cosmological reionization (Gnedin 2001; Cen & McDonald 2002; Fan et al. 2002), together with the rapid rise towards high redshifts of the neutral fractions inferred from a sample of high redshift quasars from  $5 \lesssim z \lesssim 6$  (Songaila & Cowie 2002), suggest that the IGM becomes neutral at a relatively narrow redshift interval,  $\Delta z \sim 1$ , beyond the redshifts of the most distant sources.

An alternative way of probing the reionization history is to study the temperature and polarization anisotropies of the cosmic microwave background (CMB). Both anisotropy patterns are affected by Thomson scattering of CMB photons off the free electrons in a reionized IGM (Zaldarriaga 1997). Physically, the CMB and the GP troughs probe two different stages

of reionization: the CMB is sensitive to the initial phase when  $x_{\text{H}}$  first decreases below unity, and free electrons appear; say, at redshift  $z_e$ . On the other hand, the (hydrogen) GP trough is sensitive to the late stages, when the remaining neutral hydrogen atoms are cleared away, at redshift  $z_{\text{H}}$  (Kaplinghat et al. 2003). The recent measurement by the *WMAP* (Bennett et al. 2003) satellite of the optical depth,  $\tau = 0.17 \pm 0.04$  to Thomson scattering (Kogut et al. 2003) implies a reionization redshift of  $z_e = 17 \pm 5$ , under the assumption that reionization occurs abruptly. This is to be compared to  $z_{\text{H}} \sim 6-7$ , obtained from extrapolations of the available high redshift quasar spectra at  $z \sim 6$ . If the redshift  $z_{\text{H}}$  coincided with  $z_e$ , it would imply optical depths of only  $\tau \sim 0.4-0.5$ . While the formal discrepancy between this opacity and the *WMAP* value is only at the  $\sim 3\sigma$  level, it is timely to ask the following questions: (1) *what are the physical requirements on the ionizing sources in a  $\Lambda$ CDM cosmology to produce an optical depth of  $\tau \sim 0.17$ , and (2) are these consistent with other data at  $z \lesssim 6$ ?*

In this paper, we address both of these questions. In the  $\Lambda$ CDM cosmology favored by *WMAP*,  $\sim 3$  sigma peaks of the primordial density field on mass scales of  $M \sim 10^6 M_\odot$  collapse at redshifts of  $z \sim 20$ . The onset of reionization at similar redshifts is therefore dependent on efficient formation of ionizing sources in nonlinear objects down to these low mass-scales. Early reionization can be accommodated in models of reionization in  $\Lambda$ CDM cosmologies (Shapiro, Giroux & Babul 1994; Tegmark et al. 1994; Haiman & Loeb 1997, 1998; Valageas & Silk 1999; Haiman, Abel & Rees 2000), and is indeed a natural consequence in models including a sufficient number of metal-free stars (Wyithe & Loeb 2003 and Cen 2003). If the optical depth is as high as the central value determined by *WMAP*, then future CMB polarization measurements can provide significant constraint on such models (Kaplinghat et al. 2003, see also Venkatesan 2000, 2002).

This paper is organized as follows: in § 2, we discuss the

relevant physical effects that can lead to reionization histories consistent with both the *WMAP* data and the  $z \sim 6$  quasar spectra. In § 3, we then describe a semi-analytical model that takes these effects into account, and in § 4, we derive and discuss the ionization histories in a suite of models. In § 5, we quantify constraints on the models that will be available from future polarization measurements by *WMAP* and by the Planck satellite.<sup>1</sup> Motivated by the required presence of ionizing sources at  $z \sim 20$ , in § 6 we consider the highest redshift at which the *James Webb Space Telescope* can detect these sources. Finally, we discuss our results and offer our conclusions in § 7. In this paper we adopt the background cosmological parameters as measured by the *WMAP* experiment (Spergel et al. 2003, Tables 1 and 2),  $\Omega_m = 0.29$ ,  $\Omega_\Lambda = 0.71$ ,  $\Omega_b = 0.047$ ,  $h = 0.72$  and an initial matter power spectrum  $P(k) \propto k^n$  with  $n = 0.99$  and normalization  $\sigma_8 = 0.9$ ; with the exception of § 4.6, where we consider the running index model favored by the combination of *WMAP* with other data (Spergel et al. 2003, Table 10).

## 2. SUMMARY OF RELEVANT PHYSICS AT HIGH REDSHIFTS

In the context of  $\Lambda$ CDM cosmologies, it is natural to identify the first dark matter condensations (“halos”) as the hosts of the first sources of light. A simplified picture for reionization is as follows: the gas in dark matter halos cools and turns into ionizing sources, which drive expanding ionized regions into the IGM. The volume filling factor of ionized regions then tracks the formation of dark halos. Eventually, the ionized regions percolate, and the remaining neutral hydrogen in the IGM is quickly cleared away as the ionizing background builds up. From the point of view of the large-angle CMB polarization anisotropies, what matters most is the free electron fraction  $x_e = n_e/n_{\text{tot}}$ . Accordingly, we now briefly describe the various effects that should determine the evolution of  $x_e(z)$  at high redshifts. For in-depth discussion, we refer the reader to extended reviews (Barkana & Loeb 2001; Loeb & Barkana 2001), and to reviews focusing on the roles of  $\text{H}_2$  molecules in reionization (Abel & Haiman 2000), on the effect of reionization on CMB anisotropies (Haiman & Knox 1999), and on progress in the last two years in studying reionization (Haiman 2003).

In the discussions that follow, it will be useful to distinguish dark matter halos in three different ranges of virial temperatures, as follows:

$$\begin{aligned} 100 \text{ K} &\lesssim T_{\text{vir}} \lesssim 10^4 \text{ K} && \text{(Type II)} \\ 10^4 \text{ K} &\lesssim T_{\text{vir}} \lesssim 2 \times 10^5 \text{ K} && \text{(Type Ia)} \\ &T_{\text{vir}} \gtrsim 2 \times 10^5 \text{ K} && \text{(Type Ib)} \end{aligned}$$

We will hereafter refer to these three different types of halos as Type II, Type Ia, and Type Ib halos. The motivation in distinguishing Type II and Type I halos is based on  $\text{H}_2$  molecular vs atomic H cooling (§ 2.1), whereas types “a” and “b” reflect the ability of halos to allow infall and cooling of photoionized gas (§ 2.3). While the actual values of the temperatures, and the sharpness of the transition from one category to the next is uncertain, as we argue below, each type of halo likely plays a different role in the reionization history. In short, Type II halos can host ionizing sources only in the neutral regions of the IGM, and only if  $\text{H}_2$  molecules are present; Type Ia halos can form new ionizing sources only in the neutral IGM regions, but

irrespective of the  $\text{H}_2$  abundance, and Type Ib halos can form ionizing sources regardless of the  $\text{H}_2$  abundance, and whether they are in the ionized or neutral phase of the IGM. In the following sections, we provide a summary of the various important physical effects. Much of this summary relies on existing literature; our primary difference from existing ideas is in the description of the transition from metal-free to normal stellar population (§ 2.3).

### 2.1. $\text{H}_2$ Molecule Formation

In  $\Lambda$ CDM cosmologies, structure formation is bottom-up: the earliest nonlinear dark matter halos form at low masses. Gas contracts together with the dark matter only in dark halos above the cosmological Jeans mass,  $M_J \approx 10^4$ . However, this gas can only cool and contract to high densities in somewhat more massive halos, with  $M \gtrsim M_{\text{H}_2} \equiv 10^5 M_\odot [(1+z)/11]^{-3/2}$  (i.e. Type II halos), and only provided that there is a sufficient abundance of  $\text{H}_2$  molecules, with a relative number fraction at least  $n_{\text{H}_2}/n_{\text{H}} \sim 10^{-3}$  (Haiman, Thoul & Loeb 1996; Tegmark et al. 1997). Because the typical collapse redshift of halos is a strong function of their size, the abundance of  $\text{H}_2$  molecules is potentially the most important parameter in determining the onset of reionization. For example,  $2\sigma$  halos with virial temperatures of 100K appear at  $z = 16$ , while  $2\sigma$  halos with virial temperatures of  $10^4$ K (Type Ia halos, in which gas cooling is enabled by atomic hydrogen lines) appear only at  $z = 9$ . Table 1 summarizes the collapse redshifts and masses of dark halos at these two virial temperatures. As a result, the presence or absence of  $\text{H}_2$  in Type II halos makes a factor of  $\sim 2$  difference in the redshift for the onset of structure formation, and thus potentially effects the reionization redshift and the electron scattering opacity  $\tau$  by a similar factor. In the absence of any feedback processes, the gas collecting in Type II halos is expected to be able to form the requisite amount of  $\text{H}_2$  (Haiman, Thoul & Loeb 1996; Tegmark et al 1997). However, both internal and external feedback processes can alter the typical  $\text{H}_2$  abundance (see discussion in § 2.5 below).

### 2.2. The Nature of Ionizing Sources

A significant uncertainty is the nature of the ionizing sources turning on inside halos collapsing at the highest redshifts. Three dimensional simulations using adaptive mesh refinement (AMR; Abel, Bryan & Norman 2000, 2002) and smooth particle hydrodynamics (SPH; Bromm, Coppi & Larson 1999, 2002) techniques have followed the contraction of gas in Type II halos at high redshifts to high densities. These works have shown convergence toward a temperature/density regime of  $T \sim 200$  K,  $n \sim 10^4 \text{ cm}^{-3}$ , dictated by the critical density at which the excited states of  $\text{H}_2$  reach equilibrium population levels. These results have suggested that the first Type II halos can only form unusually massive stars, with masses of at least  $\sim 200 M_\odot$ , and only from a small fraction ( $\lesssim 0.01$ ) of the available gas. Such massive stars are effective producers of ionizing radiation, making reionization easier to achieve. In addition, it is expected that the first massive stars, forming out of metal-free gas, have unusually hard spectra (Tumlinson & Shull 2000; Bromm, Kudritzki & Loeb 2001; Schaerer 2002), which is important for possibly ionizing helium, in addition to hydrogen. An alternative possibility is that a similar fraction of the gas in the first Type II halos forms massive black holes (Haiman & Loeb 1997; Bromm & Loeb 2002). These early black holes can then accrete gas, acting as “miniquasars”, and producing a hard spec-

<sup>1</sup> CMB constraints are discussed in more detail in a companion paper (paper II, Holder et al. 2003), focusing on information beyond measuring  $\tau$ , and on the possible bias in the values of  $\tau$  measured without a-priori knowledge of the reionization history.

trum extending to the soft X-rays. These soft X-rays could be important in catalyzing  $H_2$  formation (see discussion in § 2.5 below).

### 2.3. Efficiency Parameters and the Transition from Metal Free to “Normal” Stars

Another fundamental question of interest is the efficiency at which the ionizing source(s) associated with each halo eject ionizing photons into the IGM. This can be parameterized by the product  $\epsilon_* \equiv N_\gamma f_* f_{\text{esc}}$ , where  $f_* \equiv M_*/(\Omega_b M_{\text{halo}}/\Omega_m)$  is the fraction of baryons in the halo that turns into stars;  $N_\gamma$  is the mean number of ionizing photons produced by an atom cycled through stars, averaged over the initial mass function (IMF) of the stars; and  $f_{\text{esc}}$  is the fraction of these ionizing photons that escapes into the IGM. It is difficult to estimate these quantities at high-redshifts from first principles, but the numbers and discussion below can serve as a useful guide.

Although the majority of the baryonic mass in the local universe has been turned into stars (Fukugita, Hogan & Peebles 1998), the global star formation efficiency at high redshifts was likely lower. To explain a universal carbon enrichment of the IGM to a level of  $10^{-2} - 10^{-3} Z_\odot$ , the required efficiency, averaged over all halos at  $z \gtrsim 4$ , is  $f_* = 2 - 20\%$  (Haiman & Loeb 1997). However, the numerical simulations mentioned in § 2.2 above suggest that the fraction of gas turned into massive stars in Type II halos is  $f_* \lesssim 1\%$ .

The escape fraction of ionizing radiation in local starburst galaxies is of order  $\sim 10\%$ . The higher characteristic densities at higher redshifts could decrease this value (Dove et al. 2000; Wood & Loeb 2000), although there are empirical indications that the escape fraction in  $z \sim 3$  galaxies may instead be higher (Steidel, Pettini & Adelberger 2001). Radiation can also more readily ionize the local gas, and escape from the small Type II halos which have relatively low total hydrogen column densities ( $\lesssim 10^{17} \text{ cm}^{-2}$ ).

The ionizing photon yield per proton for a normal Salpeter IMF is  $N_\gamma \approx 4000$ . However, if the IMF consists exclusively of massive  $M \gtrsim 200 M_\odot$  metal-free stars, then  $N_\gamma$  can be up to a factor of  $\sim 20$  higher (Bromm, Kudritzki & Loeb 2001; Schaerer 2002). The transition from metal-free to a “normal” stellar population is thought to occur at a critical metallicity of  $Z_{\text{cr}} \sim 5 \times 10^{-4} Z_\odot$  (Bromm et al. 2001). It is natural to associate this transition with that of the assembly of halos with virial temperatures of  $> 10^4 \text{ K}$  (Type Ia halos). Type II halos are fragile, and likely blow away their gas and “shut themselves off” after a single episode of (metal-free) star-formation. They are therefore unlikely to allow continued formation of stars with metallicities above  $Z_{\text{crit}}$ . Subsequent star-formation will then occur only when the deeper potential wells of Type Ia halos are assembled and cool their gas via atomic hydrogen lines. The material that collects in these halos will then have already gone through a Type II halo phase and contain traces of metals.

As we argue in § 2.5 below, there exists an alternative, equally plausible scenario. Most Type II halos may not have formed any stars, due to global  $H_2$  photodissociation by an early cosmic soft-UV background. In this case, the first generation of metal-free stars must appear in Type Ia halos. Halos above this threshold can eject most of their self-produced metals into the IGM, but, in difference from Type II halos, can retain most of their gas (MacLow & Ferrara 1999), and can have significant episodes of metal-free starformation. These halos will also start the process of reionization by driving expanding ioniza-

tion fronts into the IGM. The metals that are ejected from Type Ia halos will reside in these photoionized regions of the IGM. As discussed in § ref:feedback below, photoionization heating in these regions suppresses gas infall and cooling, causing a pause in the formation of new structures, until larger dark matter halos, with virial temperatures of  $T_{\text{vir}} \gtrsim 2 \times 10^5 \text{ K}$  (Type Ib halos) are assembled. The material that collects in Type Ib halos will then have already gone through a previous phase of metal-enrichment by Type Ia halos, and it is unlikely that Type Ib halos can form significant numbers of metal-free stars.

The effect of a metal-free to a normal stellar population on the reionization history was studied recently by Wyithe & Loeb (2003) and Cen (2003). Both of these works assumed that rather than being tied either to a Type II→Ia or Type Ia→Ib halo transition, the switch from metal-free to normal stars occurs abruptly at a critical redshift  $z_{\text{cr}}$ . This would be justified in the picture of a uniformly increasing metal-enrichment of the IGM, and would lead to qualitatively different reionization histories from the ones we obtain below.

### 2.4. Density Fluctuations (Clumpiness) of the IGM

As the ionizing fronts propagate into the IGM, their expansion rate at high redshifts is limited by the mean recombination rate in the ionized gas (rather than simply by the ionizing luminosity). The recombination rate per unit time and volume can be written as  $\alpha_B C_{\text{HII}} \langle n_{\text{HII}} \rangle^2$ , where  $\alpha_B$  is the recombination coefficient of neutral hydrogen to its excited states ( $= 2.6 \times 10^{-13} \text{ cm}^3 \text{ s}^{-1}$  at  $T = 10^4 \text{ K}$ ),  $\langle n_{\text{HII}} \rangle$  is the mean number density of ionized hydrogen, and  $C_{\text{HII}} \equiv \langle n_{\text{HII}}^2 \rangle / \langle n_{\text{HII}} \rangle^2$  is the mean clumping factor of ionized gas. The clumping factor can be estimated by numerical simulations (Gnedin & Ostriker 1997), and in semi-analytic models (Madau et al. 1999; Chiu & Ostriker 2000; Miralda-Escudé et al. 2000; Haiman, Abel & Madau 2001; Benson et al. 2001; Wyithe & Loeb 2003). It is expected that the clumping factor rises from a value near unity to a few tens, as structures go increasingly nonlinear, between redshifts  $z = 10 - 20$ . Numerical simulations predict  $C_{\text{HII}} = 1 - 10$  at  $z > 10$ , but at high redshifts, where numerical simulations cannot resolve the Jeans mass, and the effective clumping can be increased by fluctuations on small scales (Haiman, Abel & Madau 2000), to  $C_{\text{HII}} \approx 40$  at  $z \sim 10$ . Finally, we note that whenever recombinations are fast enough to set the expansion rate of the ionization fronts, which is indeed the case in the models we consider below, it is essentially the linear combination  $\epsilon_*/C_{\text{HII}}$  that determines the evolution of the total ionized volume fraction.

### 2.5. Feedback Effects

Several feedback effects are likely to be important for reionization. There can be significant *internal* feedback in or near each ionizing source, due to the presence of supernovae (Ferrara 1998), or of the radiation field (Omukai & Nishi 1999; Ricotti, Gnedin & Shull 2002), on the local  $H_2$  chemistry. The net sign of these effects is difficult to compute, as it depends on the source properties and spectra, and on the detailed density distribution internal and near to the sources. For practical purposes of computing the global reionization history, we may, however, think of any internal feedback effect as regulating the efficiency parameter  $\epsilon_*$  defined above.

Since the universe is optically thin at soft UV ( $< 13.6 \text{ eV}$ ), and soft X-ray ( $\gtrsim 1 \text{ keV}$ ) photon energies, radiation from the earliest Type II halos can build up global backgrounds in these

bands, and provide prompt *external* feedback on the formation of subsequent structures, which are easier to follow. In particular, soft UV photons can photodissociate  $H_2$  molecules, while X-rays can promote  $H_2$  formation (Haiman, Abel & Rees 2000). The net sign of this feedback depends on the spectrum (with a critical X-ray/UV energy flux ratio of a few percent) of the earliest sources (Haiman, Abel & Rees 2000; Ciardi, Ferrara & Abel 2000; Machacek, Bryan & Abel 2001, 2003; Glover & Brandt 2003).

A second type of important feedback is that photo-ionized regions are photo-heated to a temperature of  $\gtrsim 10^4$  K, with a corresponding increase in the Jeans mass in these regions. As a result, gas from existing Type II halos is photo-evaporated (Shapiro et al. 1998; Barkana & Loeb 1999), and if the gas is kept photoionized, then Type Ia halos are subsequently prohibited from collecting gas at their centers. Gas infall and cooling in the ionized zones is suppressed in halos with virial temperatures up to  $\sim 2 \times 10^5$  K (Efstathiou 1992; Thoul & Weinberg 1995; Navarro & Steinmetz 1997). Type Ia dark matter halos that form in already ionized regions are therefore effectively excluded from contributing to reionization; in the ionized regions, new ionizing sources will have to wait until Type Ib halos build up further down in the hierarchy of structure formation.

### 3. MODELS OF REIONIZATION

In this section, we describe our semi-analytical model of the reionization process, incorporating the above effects in the simplest possible way. In these models, we track the total volume of ionized regions, assuming that ionizing sources are located inside virialized dark matter halos. Each source creates an ionized Strömberg region, which expands into the IGM at a rate dictated by the source luminosity, and by the background IGM density and clumping factor.

We adopt the mass function of virialized dark matter halos from the N-body simulations of Jenkins et al. (2001). The comoving number density  $(dn/dM)dM$  of halos at redshift  $z$  with mass  $M \pm dM/2$  is given by

$$\frac{dn}{dM}(z, M) = 0.315 \frac{\rho_0}{M} \frac{1}{\sigma_M} \frac{d\sigma_M}{dM} \exp\left[-|0.61 - \log(D_z \sigma_M)|^{3.8}\right], \quad (1)$$

where  $\sigma_M$  is the r.m.s. density fluctuation, computed on mass-scale  $M$  from the present-day linear power spectrum (Eisenstein & Hu 1999),  $D_z$  is the linear growth function, and  $\rho_0$  is the present-day total mass density.

The gas inside each virialized object is shock-heated to the virial temperature,

$$T_{\text{vir}} \approx 1800 \left(\frac{M}{10^6 M_\odot}\right)^{2/3} \left(\frac{1+z}{21}\right) \left(\frac{\Omega_0}{0.3}\right)^{1/3} \left(\frac{h}{0.7}\right)^{2/3} \left(\frac{\mu}{1.22}\right) \text{K}, \quad (2)$$

where  $\mu$  is the mean molecular weight ( $\mu = 0.60$  for ionized gas collecting in Type Ia,b halos, and  $\mu = 1.22$  for neutral gas of primordial composition, relevant for gas collecting in the shallow potentials of Type II halos).

In order to address the two global radiative feedback effects described in § 2.5 above, we separately define, and track, the total fraction of the mass in the universe that is condensed into Type II, Ia, and Ib halos:

$$F_{\text{coll,II}}(z) \equiv \frac{1}{\rho_0} \int_{M_{\text{II}}}^{M_{\text{Ia}}} dM \left(\frac{dn}{dM}\right) M, \quad (3)$$

$$F_{\text{coll,Ia}}(z) \equiv \frac{1}{\rho_0} \int_{M_{\text{Ia}}}^{M_{\text{Ib}}} dM \left(\frac{dn}{dM}\right) M, \quad (4)$$

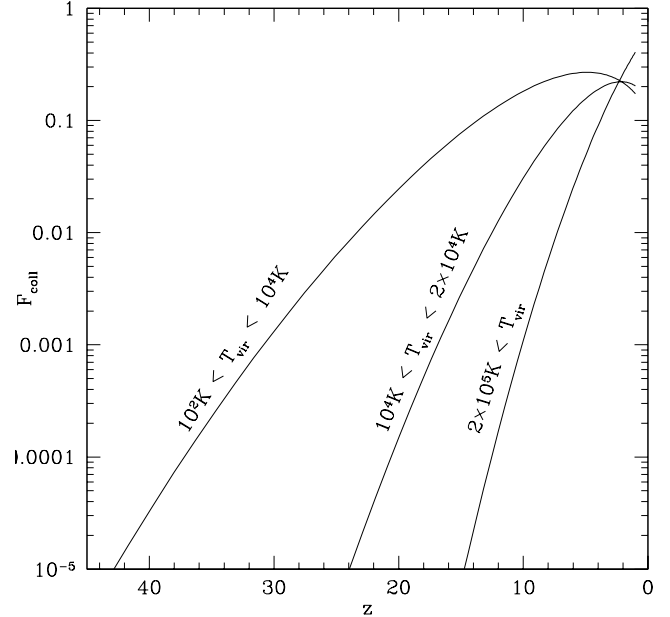


FIG. 1. — The evolution of the collapsed fraction of all baryons in halos in three different virial temperature ranges. The three different virial temperature ranges represent halos that can form ionizing sources (1) only in the neutral regions of the IGM, and only if  $H_2$  molecules are present, (2) only in the neutral IGM regions, irrespective of the  $H_2$  abundance, and (3), irrespective of the  $H_2$  abundance, and both in the ionized or neutral phases of the IGM.

and

$$F_{\text{coll,Ib}}(z) \equiv \frac{1}{\rho_0} \int_{M_{\text{Ib}}}^{\infty} dM \left(\frac{dn}{dM}\right) M, \quad (5)$$

where the halo masses  $M_{\text{II}} = M_{\text{II}}(T_{\text{II}}, z)$ ,  $M_{\text{Ia}} = M_{\text{Ia}}(T_{\text{Ia}}, z)$ , and  $M_{\text{Ib}} = M_{\text{Ib}}(T_{\text{Ib}}, z)$  are obtained from equation (2) for the temperatures  $T_{\text{II}} = 100$  K,  $T_{\text{Ia}} = 10^4$  K and  $T_{\text{Ib}} = 2 \times 10^5$  K. Our results below are insensitive to the upper limit in equation (5). The collapsed fractions are shown in Figure 1. The time derivatives of equations (3)-(5), in turn, represent the rates at which mass is condensing into nonlinear halos. At low redshifts, the derivatives can turn negative; which represents the decrease in the number of halos as they merge into larger systems. This does not significantly effect our results at the high redshifts we consider  $z \gtrsim 6$ .

We assume that each halo represents a single cosmological “reionizing source”, which drives an expanding ionized region into the IGM. For each initial source redshift, we solve the equation of motion for the ionization front,  $R_i$ ,

$$\frac{dR_i^3}{dt} = 3H(z)R_i^3 + \frac{3\dot{N}_\gamma}{4\pi\langle n_H \rangle} - C_{\text{HII}}\langle n_H \rangle \alpha_B R_i^3, \quad (6)$$

where  $H(z)$  is the Hubble constant at  $z$ ,  $\alpha_B = 2.6 \times 10^{-13} \text{ cm}^3 \text{ s}^{-1}$  is the recombination coefficient of neutral hydrogen to its excited states at  $T = 10^4$  K, and  $C_{\text{HII}}$  is the mean clumping factor of ionized gas within  $R_i$  as discussed in § 2.4 above. The first term in equation (6) accounts for the Hubble expansion, the second term accounts for the ionizations by newly produced photons, and the last term describes recombinations (Shapiro & Giroux 1987; Haiman & Loeb 1997).

In equation (6),  $\dot{N}_\gamma$  represents the emission rate of ionizing photons from a single halo. For a stellar population with a Salpeter IMF (initial mass function) undergoing a burst of star

formation at a metallicity equal to 2% of the solar value (Leitherer et al. 1999), we find that the rate is well approximated by

$$\dot{N}_\gamma(t) = \begin{cases} \dot{N}_0 & (t \leq 10^{6.5} \text{ yr}) \\ \dot{N}_0(t/10^{6.5} \text{ yr})^{-4.5} & (t > 10^{6.5} \text{ yr}), \end{cases} \quad (7)$$

where  $\dot{N}_0 = 3.7 \times 10^{46} \text{ s}^{-1} \text{ M}_\odot^{-1}$  (per  $\text{M}_\odot$  of stellar mass). Over the lifetime of the population, this produces  $\approx 4000$  ionizing photons per stellar proton. In practice, the injection of ionizing photons is nearly instantaneous compared to the expansion timescale even at redshift  $z \sim 20$ , and our results are insensitive to the adopted lightcurve (an assumption that remains justified for an IMF biased to more massive stars).

In order to investigate the various physical effects outlined in § 2, we define separate star-formation efficiencies,  $\epsilon_{\text{II}}$ ,  $\epsilon_{\text{Ia}}$ , and  $\epsilon_{\text{Ib}}$  for Type II, I, and Ib halos, respectively. In order to allow for a negative radiative feedback by the soft UV background on the  $\text{H}_2$  abundance, we consider a redshift  $z_{\text{UV}}$  below which  $\epsilon_{\text{II}} = 0$ , so that Type II halos are excluded from contributing to reionization. In reality, rather than dropping to zero, the efficiency in Type II halos should roughly remain at a constant “steady state” value, set by the level of starformation that can just be maintained against the  $\text{H}_2$  photo-dissociation implied by this starformation (Haiman, Abel & Rees 2000). Retaining this level of starformation in our models would have a relatively small effect on our results.

For the sake of simplicity, we adopt a constant clumping factor  $C_{\text{HII}}$ . While the clumping factor does evolve with redshift, at  $z \gtrsim 10$ , this could be absorbed as a factor of  $\sim 10$  decrease in the efficiencies  $\epsilon$  down to this redshift. Including the evolution of the clumping factor with redshift would be necessary in order to model the evolution of the neutral fraction at  $5.5 \lesssim z \lesssim 6.5$ , necessary to interpret its sharp rise in the observed high-redshift quasar spectra. However, semi-analytical models (Haiman & Loeb 1997, 1998) and numerical simulations (Gnedin & Ostriker 1997; Gnedin 2001; Razoumov et al. 2002;) have shown that even though the entire process of reionization can last for an extended period, the rapid evolution in the neutral fraction, caused by the sudden buildup of the radiation background once the ionized regions percolate, follows the percolation epoch within a short redshift interval  $\Delta z < 1$ . We will require only that our model indicate a “second reionization” epoch at  $z \sim 7$ , and defer detailed modeling of the neutral fraction to a future paper.

Combining the abundance of the ionizing sources (eq. 1) with the ionized volume associated with each source (eq. 6), we can compute the volume filling fraction of the ionized regions as a function of redshift. The ionized volume associated with a halo of mass  $M$  scales linearly with its mass and with the efficiency factor  $\epsilon$ , namely  $V_{\text{HII}}(z_{\text{on}}, z, M) = (4\pi R_1^3/3) = \epsilon M \times \tilde{V}_{\text{HII}}(z_{\text{on}}, z)$ , where  $\tilde{V}_{\text{HII}}(z_{\text{on}}, z)$  is the ionized volume per unit mass and unit efficiency, and  $R_1$  is the solution of equation (6). The HII filling factor  $F_{\text{HII}}(z)$  is then obtained from the collapsed gas fractions as

$$F_{\text{HII}}(z) = \rho_b(z) \int_{\infty}^z dz' \left\{ \epsilon_{\text{Ib}} \frac{dF_{\text{coll,Ib}}}{dz}(z') + [1 - F_{\text{HII}}(z')] \times \left[ \epsilon_{\text{Ia}} \frac{dF_{\text{coll,Ia}}}{dz}(z') + \epsilon_{\text{II}} \frac{dF_{\text{coll,II}}}{dz}(z') \right] \right\} \tilde{V}_{\text{HII}}(z', z), \quad (8)$$

where  $\rho_b = \Omega_b \rho_{\text{crit}}$  is the average baryonic density and  $\rho_{\text{crit}}$  is the critical density of the universe. In the second term on the right hand side of equation (8), we have explicitly included a

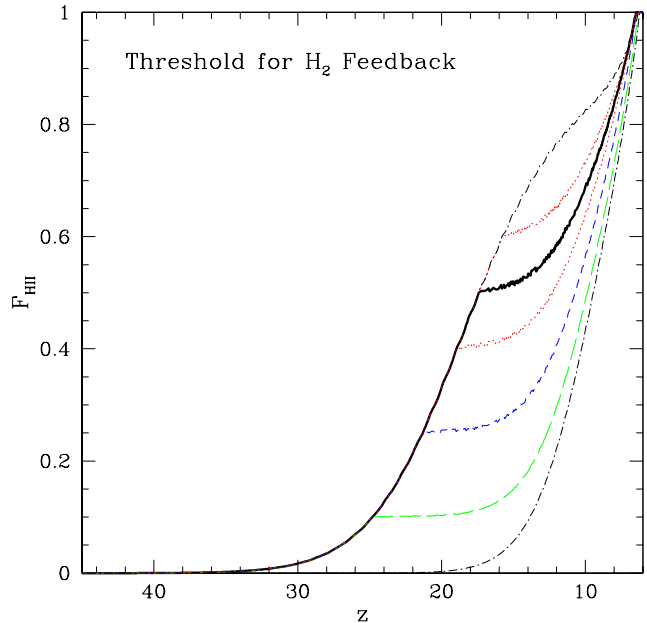


FIG. 2.— The evolution of the ionized fraction of all baryons. The thick solid curve corresponds to our fiducial model described in § 4.1. The other curves indicate variations in the importance of  $\text{H}_2$  photodissociation feedback, from no feedback (top dot-dashed curve), to strong feedback that effectively excludes Type II halos from contributing to reionization (bottom dot-dashed curve). The pair of dotted curves bracket a range  $\Delta\tau = \pm 0.01$  around the fiducial model; the short and long-dashed curves correspond to reductions in  $\tau$  by  $\Delta\tau = 0.03$  and  $0.06$ , respectively (see § 4.2 for discussion).

factor  $(1 - F_{\text{HII}})$ , which takes into account the fact that new ionizing sources should appear in Type II and Type Ia halos only in regions which have not yet been ionized.

Equations (1-8) determine the evolution of the ionized fraction. Note that equation (8) is implicit, and, in practice, has to be solved numerically by starting at high redshift ( $z = 60$ ), and taking sufficiently small negative redshift steps (we found  $\Delta z \approx 0.001$  to be adequate in most of the models we studied). In summary, our model has five parameters: the clumping factor  $C_{\text{HII}}$ , the overall efficiencies,  $\epsilon_{\text{II}}$ ,  $\epsilon_{\text{Ia}}$ ,  $\epsilon_{\text{Ib}}$ , and the redshift  $z_{\text{UV}}$  at which  $\text{H}_2$  dissociative feedback sets in. Since variations in the clumping factor are nearly degenerate with changes in the efficiency parameters, in all of our models we fix  $C_{\text{HII}} = 10$  (alternatively, adopting a redshift-dependent clumping factor from the works discussed in § 2.4 would only case a “tilt” in the reionization histories we derive below). We therefore have four “free” parameters. Current CMB constraints are not sufficiently accurate to converge on a “best-fit” model, and our main purpose here is to be able to study the various physical effects outlined in § 2 above. Nevertheless, the hope (as we attempt to demonstrate in § 5 below) is that eventually, CMB polarization data *will* provide constraints on parameters of models similar to the one described here, while simultaneously delivering constraints on cosmological parameters.

#### 4. POSSIBLE REIONIZATION HISTORIES

In this section, we present a suite of models, designed to investigate the various effects summarized in § 2 above. Note that more realistic calculations would explicitly have to couple the star formation efficiency with radiative feedback processes (as attempted in part by Haiman, Abel & Rees 2000, Glover &

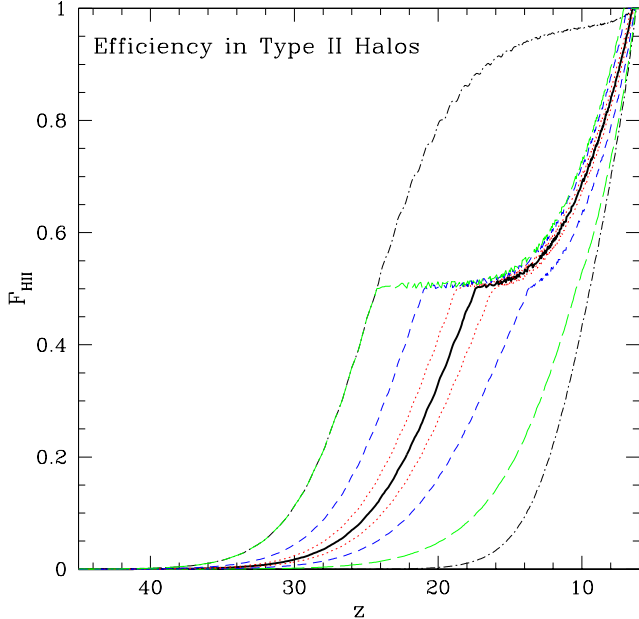


FIG. 3.— The evolution of the ionized fraction of all baryons, with the thick solid curve showing the fiducial model as in Figure 2. The other curves indicate variations in the efficiency parameter  $\epsilon_{\text{II}}$  in Type II halos. As in Figure 2, the pairs of dotted, short-dashed, and long-dashed curves bracket a range of  $\Delta\tau = \pm 0.01, 0.03,$  and  $0.06$  around the fiducial model. The required changes in the efficiencies are described in the text. The bottom dot-dashed curve assumes Type II halos do not form stars, and the top dot-dashed curve assumes that there is no  $\text{H}_2$  photodissociation feedback (see § 4.3 for discussion).

Brandt 2003, and Cen 2003). In the present models, we explicitly track only the ionized fraction of hydrogen. For the purpose of computing the electron scattering optical depth, we assume that the HII and HeII fractions are identical, so that the extra electrons from HeII increase the opacity by a factor of 1.08. A HeII to HeIII transition appears to be taking place at the low redshift  $z \sim 3$  (Miralda-Escudé 2001). While some HeIII could be present at high redshifts, for realistic spectral slopes of the ionizing sources, the extra electrons from HeIII regions add corrections to  $\tau$  at the  $\lesssim 10\%$  level.

#### 4.1. Fiducial Model

As discussed above, in order to match inferences from the  $z < 6$  quasar spectra, we require that a percolation takes place at redshift  $z \sim 7$ . A second motivation for requiring a percolation near  $z \sim 7$  is the high observed temperature of the IGM at  $z \sim 4$ : if the percolation occurred too early, the IGM would cool to temperatures that may be too low by  $z \approx 4$  (Hui & Haiman 2003). We find that this effectively fixes the efficiencies  $\epsilon_{\text{Ia}} = \epsilon_{\text{Ib}} = 80$  (if they are postulated to have the same value). Accordingly, in our fiducial model, we adopt these values. Note that these values are quite reasonable: for a normal stellar population,  $N_\gamma = 4000$ , and we may break down the efficiency into  $f_* = 0.2$  and  $f_{\text{esc}} = 0.1$ . With  $\epsilon_{\text{Ia}}$  and  $\epsilon_{\text{Ib}} = 80$  fixed, we have only  $z_{\text{uv}}$  and  $\epsilon_{\text{II}}$  to vary. In our fiducial model, Type II halos host metal-free stars from a small fraction ( $f_* = 0.005$ ) of the available gas, but the stars are, on average, 10 times more efficient ionizing photon producers ( $N_\gamma = 40000$ ), and all of their ionizing radiation escapes into the IGM ( $f_{\text{esc}} = 1$ ). This results in the overall efficiency of  $\epsilon_{\text{II}} = 200$ . We then finally adopt a redshift  $z_{\text{uv}} = 17$  for the onset of  $\text{H}_2$ -photodestruction, which

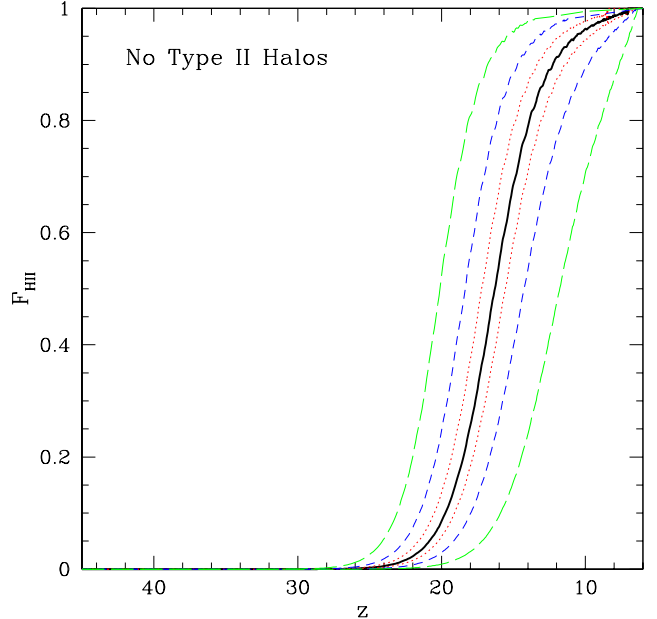


FIG. 4.— This figure assumes that  $\text{H}_2$  feedback effectively shuts off starformation in all Type II halos, and therefore Type Ia halos form metal free stars, but Type Ib halos form normal stars. The thick solid curve shows a new fiducial model that has the  $\tau = 0.17$ . This requires increasing the efficiencies in Type Ia halos by a factor of 60 relative to the fiducial models in Figures 2 and 3. The pairs of dotted, short-dashed, and long-dashed curves bracket a range of  $\Delta\tau = \pm 0.01, 0.03,$  and  $0.06$  around this new fiducial model. Note we keep the efficiency in Type II halos fixed, and percolation in all models is achieved only at  $z \sim 6$ . This can lead to consistency with inferences from  $z \sim 6$  SDSS quasar spectra (see § 4.4 for discussion).

allows Type II halos to ionize  $\sim$  half of the volume of the IGM. By construction, this model produces an optical depth  $\tau = 0.17$ , the central value in the range allowed by *WMAP*. In what follows, we separately vary each parameter – this will explicitly clarify the dependence of the reionization history and of  $\tau$  on each of our parameters.

#### 4.2. When does $\text{H}_2$ dissociation feedback set in?

The redshift at which any  $\text{H}_2$  dissociation sets in is determined by the spectra of the light sources in Type II halos, and the intensity of the X-ray and soft UV backgrounds. According to Haiman, Abel & Rees (2000), the choice of  $z_{\text{uv}} = 17$ , resulting in Type II halos ionizing  $\sim$  half of the IGM volume, would be consistent with an X-ray/UV background energy flux ratio of a few percent. We here simply parameterize this feedback with the redshift of its onset,  $z_{\text{uv}}$ . The reionization history in our fiducial model is shown by the thick solid curve in Figure 2. The other curves in this figure show variations in  $z_{\text{uv}}$  away from the fiducial model, which correspond to changes  $\Delta\tau = 0.01, 0.03,$  and  $0.06$ . The level of the constraint that will be provided by Planck corresponds approximately to  $\Delta\tau = 0.01$  (although Planck will have information beyond a measurement of  $\tau$ , see discussion in § 5 below and in paper II). As the dotted curves in the figure show, at the level of the Planck constraint,  $z_{\text{uv}}$  could be determined to a precision of  $\Delta z_{\text{uv}} \approx \pm 1.5$ . Note that even in the absence of any  $\text{H}_2$  destruction (upper dot-dashed curve), the opacity can only be increased to  $\tau \sim 0.185$ .

#### 4.3. How different is the overall efficiency in Type II halos?

In our fiducial model, we have adopted a ratio  $\epsilon_{\text{II}}/\epsilon_{\text{Ia}} = 2.5$ , determined by the transition from metal-free to normal stars. In Figure 3, we consider variations in  $\epsilon_{\text{II}}$ . We show results for values of  $\epsilon_{\text{II}}$  that result in changes of  $\pm\Delta\tau = 0.01, 0.03, \text{ and } 0.06$  (dotted, short-dashed, and long-dashed curves, respectively). In each case, we adjust the value of  $z_{\text{UV}}$  so that the Type II halos always ionize  $\sim$  half of the volume (this approximately mimics fixing the radiation intensity at which  $\text{H}_2$  feedback sets in). The value of  $\epsilon_{\text{II}}$  for these six curves, from bottom to top, are  $\epsilon_{\text{II}} = 20, 80, 120, 280, 520, \text{ and } 1400$ . The last value still represents a relatively modest factor of  $\sim 7$  increase in the combined efficiencies, and is within the range of uncertainties. The Planck-level constraints represent  $\sim 50\%$  changes in  $\epsilon_{\text{II}}$ . The bottom dot-dashed curve shows the case of no starformation in Type II halos ( $\epsilon_{\text{II}} = 0$ ; this is equivalent to  $z_{\text{UV}} \gtrsim 35$ , shown by the bottom curve in Figure 2). The top dot-dashed curve shows the highest efficiency case, but assuming no  $\text{H}_2$  dissociation. In this model,  $\tau = 0.29$ , which would be ruled out at the  $\sim 3\sigma$  level by the current *WMAP* results.

#### 4.4. Are $\text{H}_2$ molecules required to produce large $\tau$ ?

In Figure 4, we assume that  $\text{H}_2$  feedback effectively shuts off starformation in all Type II halos. As a result, Type Ia halos form metal-free stars, and, motivated by the arguments in § 2.3, we assume that the transition to normal stellar populations took place in Type Ib halos (and we set  $\epsilon_{\text{Ib}} = 80$ ). We then revise our fiducial model and find that  $\epsilon_{\text{Ia}} = 4800$  is required to produce  $\tau = 0.17$ , implying an overall efficiency difference of a factor of 60 between Type Ia and Ib halos (shown by the solid curve). The main conclusion from Figure 4 is that  $\tau = 0.17$  can be achieved without  $\text{H}_2$  molecules, but this requires a boost in efficiencies by this factor. This would require, in turn, in addition to the maximum factor of  $\sim 20$  caused by switching from metal-free to normal stars, that the escape fraction or starformation efficiency in Type Ia halos was a factor of  $\sim 3$  higher (or else that the clumping factor decreases by the same factor from  $z \sim 15$  to  $z \sim 10$ ). Another important feature apparent from Figure 4 is that the reionization history is qualitatively different from those shown in Figures 2 and 3. As we discuss in § 5 below, future CMB polarization measurements can distinguish between the two scenarios at high significance. As in the previous figures, we also show the  $\pm\Delta\tau = 0.01, 0.03, \text{ and } 0.06$  “contours”, which correspond (bottom to top curves) to  $\epsilon_{\text{Ia}} = 480, 1600, 3200, 8000, 16000, 48000$ . Planck-level constraints on  $\epsilon_{\text{Ia}}$  are at the  $\sim 50\%$  level. It is worth pointing out that in the models shown in Figure 4, Type Ia sources are self-limiting by photo-heating feedback (shown by the flattening of the ionization histories below  $z \lesssim 12$ ) and it is the Type Ib sources that eventually cause percolation at  $z \sim 6.5$  in all models, regardless of the efficiency in Type Ia sources.

#### 4.5. Constraints on efficiencies from the percolation epoch

In our models, Type Ib halos form last, and must be responsible for the eventual percolation of the ionized regions. As argued above, to be consistent with inferences from  $z \lesssim 6$  quasar spectra, this percolation epoch cannot be at  $z \gtrsim 7$ . It is interesting to ask, then: what is the allowed efficiency range in Type Ib halos? To address this question, we consider the fiducial model defined in § 4.1, and we vary  $\epsilon_{\text{Ia}} = \epsilon_{\text{Ib}}$ . The resulting reionization histories for variations that cause  $\pm\Delta\tau = 0.01, 0.03, \text{ and } 0.06$  are shown in Figure 5. The figure shows that in high-efficiency models (corresponding to  $\Delta\tau \gtrsim 0.03$ , or  $\epsilon_{\text{Ib}} \gtrsim 1200$ ), percola-

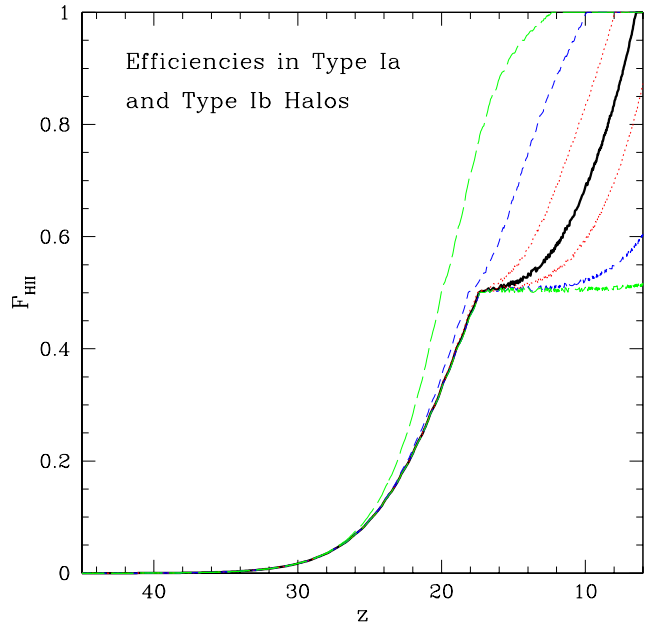


FIG. 5.— The evolution of the ionized fraction of all baryons, with the thick solid curve showing the fiducial model as in Figure 2. The other curves indicate variations in the star formation efficiency in Type Ia and Ib halos. The pairs of dotted, short-dashed, and long-dashed curves bracket a range of  $\Delta\tau \pm 0.01, 0.03, \text{ and } 0.06$  around the fiducial model, as in Figure 3 (see § 4.5 for discussion).

tion occurs at too high redshifts. Similarly, models with too low efficiencies ( $\Delta\tau \lesssim -0.01$ , or  $\epsilon_{\text{Ib}} \lesssim 30$ ) are ruled out as they fail to reionize the universe by redshift  $z \sim 6$ . The low-redshift observations by themselves therefore constrain the efficiencies in Type Ib halos to within a range of a factor of  $\sim 30$ .

#### 4.6. The running spectral index *WMAP* model

When combined with other large scale structure data, the *WMAP* results favor, at the  $\sim 2\sigma$  level, a non-scale-invariant primordial power spectrum with a running spectral index (Spergel et al. 2003). This model has much less small scale power than the best-fit *WMAP*-only model. It is interesting to ask whether  $\tau = 0.17$  can still be achieved in the running index model without  $\text{H}_2$  molecular cooling (Spergel et al. 2003). To address this question, we consider the fiducial model defined in § 4.4, but use the cosmological parameters listed in Table 10 of Spergel et al. (2003). We then increase  $\epsilon_{\text{Ia}}$  until  $\tau = 0.17$  is achieved. In Figure 6, we show the reionization history in this model, which requires boosting the efficiencies by a factor of 3000, to  $\epsilon_{\text{Ia}} = 2.5 \times 10^5$ . This model must unrealistically assume that all the gas turns into stars (and gets recycled  $\sim 3$  times), all of the ionizing radiation escapes into the IGM, the clumping factor is  $C_{\text{HII}} = 1$ , and adopt the maximum factor of  $\sim 20$  in the increase in ionizing photon production rates in massive, metal-free stars. The dotted, short-dashed, and long-dashed curves assume  $\epsilon_{\text{Ia}} = 80000, 20000, \text{ and } 9000$ , corresponding to decreasing  $\tau$  by  $\Delta\tau = -0.01, -0.03, \text{ and } -0.06$ , respectively, and showing that the lack of molecules could still be consistent with the lower range of  $\tau$  allowed in the running index model. Allowing for Type II halos (assuming no  $\text{H}_2$  feedback) we find that a relatively more realistic  $\epsilon_{\text{II}} = 4000$  is required to produce  $\tau = 0.17$ .

#### 4.7. Summary

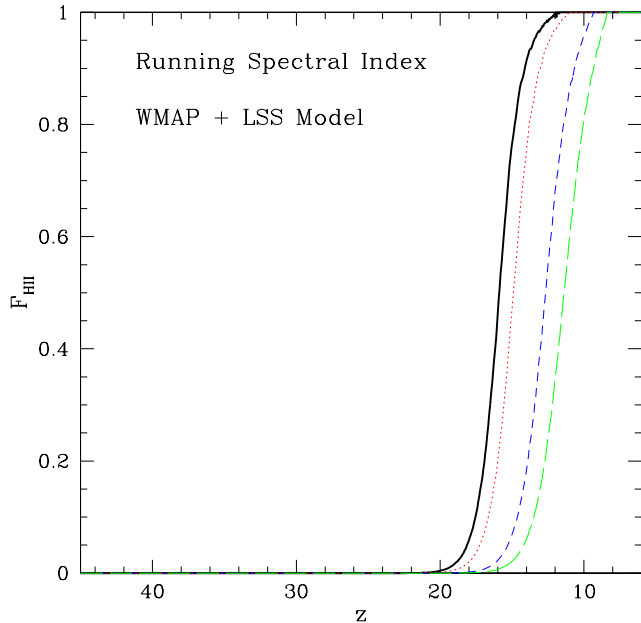


FIG. 6.— This figure replaces the best fit power law *WMAP* cosmological model by the best fit model that allows a running spectral index and combines *WMAP* and other datasets (Table 10 in Spergel et al. 2003). In this model, small-scale power is significantly reduced. The thick solid curve shows a new fiducial model that assumes no star-formation in Type II halos, and has  $\tau = 0.17$ . This requires boosting the efficiency by an unrealistic factor of 3000 relative to our fiducial model in the power-law cosmology. The dotted, short-dashed, and long-dashed curves correspond to lower efficiencies, and reduced values of  $\tau$  by  $\Delta\tau = -0.01$ ,  $-0.03$ , and  $-0.06$ , respectively (see § 4.6 for discussion).

The physics of reionization is rich in features that can naturally lead to distinctive ionization histories. These features can arise because of (1) the different types of coolants in Type II and Type I halos, (2) the different response of different halos to radiative feedback on the  $H_2$  chemistry, and to photoionization feedback on gas infall, and (3) the different efficiencies expected in metal-free and normal stellar populations. We generically find that no simple model fits both the *WMAP* data and the constraint from  $z \lesssim 6$  quasar spectra requiring that an episode of percolation occur near  $z \lesssim 7$ . Nevertheless, a range of interesting, physically motivated reionization histories is allowed by current data. We find that the ionized fraction  $F_{\text{HII}}(z)$  in these models evolves monotonically with redshift, except under the assumption of a uniformly increasing metal-enrichment of the IGM, and a sudden transition from metal-free to “normal” stars at some redshift  $z_{\text{cr}}$  (see discussion in next section, and also Wyithe & Loeb 2003 and Cen 2003).

##### 5. CONSTRAINTS FROM FUTURE CMB ANISOTROPY MEASUREMENTS

All models shown in Figures 2-6 in the previous section are consistent with the optical depth  $\tau = 0.17 \pm 0.04$  measured in the current *WMAP* data. These figures also give an indication of constraints that will be available in the future on reionization models – by showing variations in each model parameter that cause changes as small as  $\Delta\tau = \pm 0.01$  in the electron scattering optical depth. While the constraints on single parameters are impressive at this  $\Delta\tau$ , considering one parameter at a time will clearly be only the first crude step in attempts to

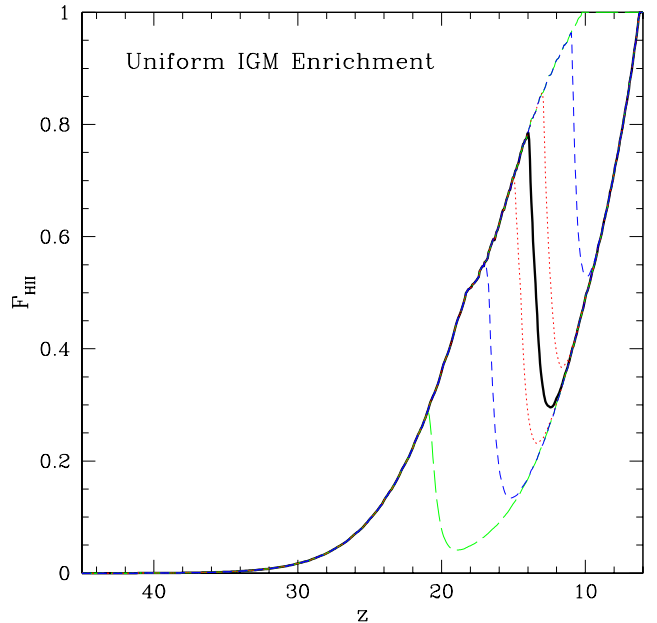


FIG. 7.— This figure addresses the hypothesis that a transition from metal free to normal star formation takes place abruptly at a fixed redshift  $z_{\text{cr}}$ , accompanied by a sudden decrease by a factor of  $f_{\text{cr}}$  in the ionizing photon production rates. The thick solid curve shows a model that has  $\tau = 0.17$ ; this is achieved by  $z_{\text{cr}} = 14$  and  $f_{\text{cr}} = 20$ . The pairs of dotted, short-dashed, and long-dashed curves bracket a range of  $\Delta\tau \pm 0.01$ ,  $0.03$ , and  $0.06$  around this model by changing  $z_{\text{cr}}$ .

understand the reionization history. Eventually, a full degeneracy study, involving simultaneous variations of all reionization model parameters, together with cosmological parameters, will be needed. While such a study is not yet called for by the *WMAP* data, our results indicate that this will be *necessary* for Planck (see paper II for in-depth discussion).

Such future studies will utilize information in the CMB polarization and temperature power spectra beyond the value of the optical depth  $\tau$ . Indeed, the lack of our a-priori knowledge of the reionization history would bias estimates of  $\tau$  itself, and would be the limiting factor in determining  $\tau$  from Planck data (see paper II). Here we consider the question: *how useful is the information beyond the measurement of  $\tau$  in constraining reionization histories?*

To address this question, we here consider three different models that have the same value of  $\tau = 0.17$ . Two of these models are the fiducial models defined in § 4.1 and § 4.4, and shown by the solid curves in Figures 2 and 4; hereafter referred to as models (A) and (B). The electron scattering in model (A) extends to redshifts higher than in model (B), and, as a result, will produce polarization anisotropy on smaller angular scales (larger spherical harmonic index  $\ell$ ). For sake of illustration, we consider a third model, similar to those proposed by Wyithe & Loeb (2003) and Cen (2003). This is a variant of model (A), in which we assume that a transition from metal free to normal stellar populations takes place abruptly at a fixed redshift  $z_{\text{cr}}$ , accompanied by a sudden decrease by a factor of  $f_{\text{cr}}$  in the ionizing photon production rates. In terms of our model parameters,  $\epsilon_{\text{II}} = \epsilon_{\text{Ia}} = \epsilon_{\text{Ib}} = 80$  at  $z < z_{\text{cr}}$  and  $\epsilon_{\text{II}} = \epsilon_{\text{Ia}} = \epsilon_{\text{Ib}} = 80f_{\text{cr}}$  at  $z \geq z_{\text{cr}}$ . We find that  $z_{\text{cr}} = 14$  and  $f_{\text{cr}} = 20$  results in  $\tau = 0.17$ ; this model is shown in Figure 7 (together with models with  $z_{\text{cr}} = 10, 11, 13, 15, 17$ , and  $21$ , which bracket the  $\Delta\tau \pm 0.01$ ,



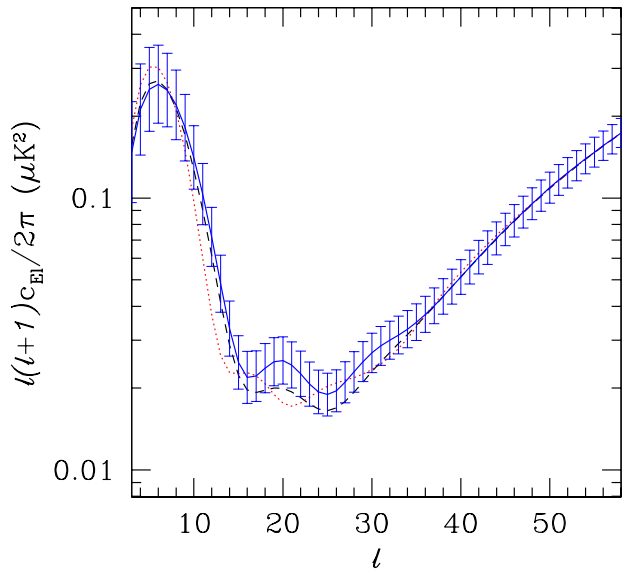


FIG. 8.— The large-angle E-mode polarization anisotropies in three different models. The dashed, dotted, and solid curves correspond to the solid curves in Figures 2, 4, and 7, respectively. All three models produce the same electron scattering opacity  $\tau = 0.17$ . Cosmic variance error bars are shown around the solid curve, in bins of  $\Delta\ell = 1$ . The three curves are statistically distinguishable in a cosmic variance limited experiment at  $> 4\sigma$  significance. Planck can only distinguish the dashed and the solid curves at  $\sim 1.6\sigma$ , but can distinguish the other two pairs of models  $> 3\sigma$  (see Table 2).

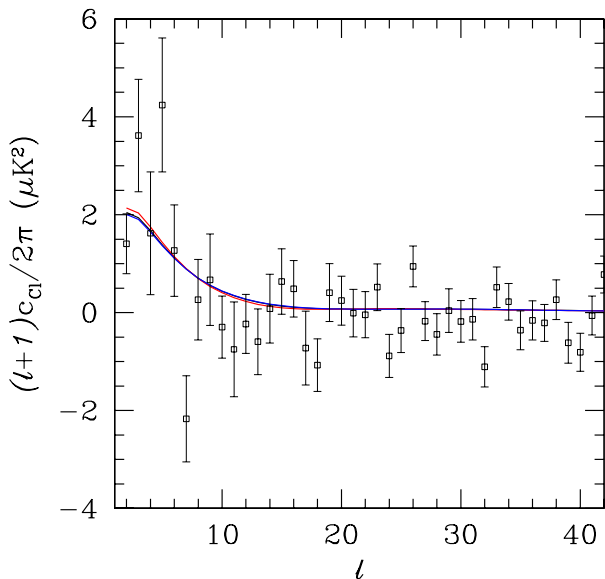


FIG. 9.— The same three models as in Figure 8, but the temperature-polarization cross-correlation is shown. The three models are nearly indistinguishable.

0.03, 0.06 range around  $\tau = 0.17$ ). Our motivation to reconsider this model, hereafter referred to as model (C), is the distinctly different shape of the reionization history.

We modified CMBFast<sup>2</sup> (Seljak & Zaldarriaga 1996) to use the ionization histories from models (A), (B) and (C) to generate temperature, polarization, and cross-correlation anisotropy power spectra,  $C_{T\ell}$ ,  $C_{E\ell}$  and  $C_{c\ell}$  respectively. The resulting EE and TE power spectra are shown by the dashed, dotted, and solid curves in Figures 8 and 9, respectively. In Figure 8, we show cosmic variance error bars in bins of  $\Delta\ell = 1$  around model (C), and in Figure 9, we overlay the *WMAP* data. The models are nearly indistinguishable in the TE power spectra, but are clearly different in the EE spectrum: model (A) is biased to lower  $\ell$  than model (B), and model (C) has excess power at small angular scales.

We next calculate the likelihood between pairs of models, using all three (EE, TE, and TT) power spectra, and a  $\Delta\bar{\chi}^2$  statistic defined in paper II (see also Kaplinghat et al. 2003). As apparent from Figures 8 and 9, nearly all of the distinguishing power comes from the E-mode polarization anisotropy alone. In Table 2, we show the significance at which pairs of models can be distinguished in the future by (1) 2-year of *WMAP* data (2) Planck, and (3) an “ultimate” cosmic variance limited experiment. The details of folding the instrumental characteristics of *WMAP* and Planck into our calculations are described in paper II.

The three curves are statistically distinguishable in a cosmic variance limited experiment at  $> 4\sigma$  significance. Planck can only distinguish models (A) and (C) at  $\sim 1.6\sigma$ , but can distinguish the other two pairs of models at  $> 3\sigma$  significance (see Table 2). It is also interesting to ask how poor a fit a “one-step” reionization model would be to real data realized from a more complex history? This issue is discussed in detail in paper II; for sake of completeness, we quote here only the difference of model (A) from one-step reionization models. We find likelihoods of  $\Delta\bar{\chi}^2$  of 0.3, 16, and 60, for 2-yr *WMAP* data, Planck, and a cosmic variance limited experiment, respectively.

In summary, our results suggest that for the physically motivated reionization histories discussed in this paper, the Planck satellite will be able to rule out both a simple 1-step reionization model, and also several “wrong” physically motivated models, at high statistical significance.

## 6. CAN JWST DETECT THE SOURCES OF REIONIZATION?

A broad conclusion that can be drawn from the *WMAP* results, reinforced in this paper, is that UV sources exist at very high redshifts ( $z \sim 20$ ). This, by itself, is a significant new discovery, and it raises the question of whether we will be able to directly detect these sources. Here we consider the capabilities of the *James Webb Space Telescope (JWST)*: what is the “limiting redshift” out to which *JWST* will be able to detect the sources of reionization? We here answer this question with a simple calculation, as follows. Consider a halo of mass  $M$  at redshift  $z$ . The number of halos  $N(> M)$  with mass above  $M$  at redshift  $z \pm dz/2$  that could be visible within a solid angle  $\Delta\Omega$  and redshift range  $\Delta z$  is given by

$$N(> M) = \Delta\Omega \times \Delta z \times f_{\text{on}} \times \left[ \frac{dV}{dzd\Omega}(z) \int_M^\infty dM' \frac{dn}{dM'} \right], \quad (9)$$

where  $dV/dzd\Omega$  is the cosmological volume element,  $dn/dM$  is the halo mass function from Jenkins et al. (2001), and  $f_{\text{on}}$  is the fraction of the time the halo spends at a luminosity detectable by *JWST*. We assume the sources live for  $t_s = 3 \times 10^6$  years (approximately the main sequence lifetime for massive

<sup>2</sup> available at <http://www.physics.nyu.edu/matasz/CMBFAST/online.html>

stars, both normal and metal-free, and a conservative estimate for the bright phase of mini-quasar activity). In this case,  $f_{\text{on}} \approx t_s/t(z) \approx 0.006-0.02$  at redshifts  $z = 10-20$  (where  $t(z)$  is the age of the universe at redshift  $z$ ).

The sensitivity expected to be reached in a  $5 \times 10^4$  second exposure “*JWST* Deep Field”, with the current 6m diameter telescope design, in the  $0.6-5\mu\text{m}$  band ( $S/N=5$ ), with the Near Infrared Camera (NIRCam) is  $\sim 1\text{nJy}$ . We require that there should be at least 100 sources visible down to this depth in the  $\Delta\Omega = 10 \text{ arcmin}^2$  field of view of NIRCam, and in  $\Delta z \approx 2$ . To predict the luminosities, consistent with our reionization models, we make the assumption that in a halo of mass  $M$ ,  $\sim 10\%$  of the gas turns into stars with a normal Salpeter IMF. We use the population synthesis models of Leitherer et al. (1999) to predict the observed spectra (at a metallicity of  $Z = 0.02$ ). We ignore wavelengths shorter than  $1215(1+z)\text{\AA}$ , because of the strong GP trough expected at high redshifts, and compute the average flux in the unobscured fraction of the  $0.6-5\mu\text{m}$  wavelength range.

Under these assumptions, we find that a halo of mass  $2 \times 10^8 M_\odot$  at redshift  $z = 14$  would have an average flux of  $\sim 1\text{nJy}$  in the unobscured  $1.8-5\mu\text{m}$  range, detectable with NIRCam. Such a halo represents a  $3\sigma$  object at  $z = 14$  in the *WMAP* cosmology, and with our derived duty-cycle of  $f_{\text{on}} = 0.01$  there should be 100 such sources detectable at any given time in  $10 \text{ arcmin}^2$ . This halo would have a virial temperature of  $\sim 2 \times 10^4 \text{ K}$ , justifying the assumed star formation efficiency of 10% (larger than is expected in Type II halos). As we argued above in § 2.3, it is possible that most stars are still metal-free in Type Ia halos at these high redshifts. Although metal free stars produce more ionizing photons than normal stars, owing to their high effective temperatures, they are fainter at the *JWST* wavelengths than normal stars. This, however, is likely offset by the steep IMF expected from a metal-free stellar population. We conclude that *JWST* could directly detect the sources of reionization, out to redshifts as high as  $z \sim 14$ ; these sources would be sufficiently bright to allow follow-up spectroscopy with NIRSpec on *JWST*. The sources could also be discovered in line emission, either in the  $\text{H}\beta$  line (Oh 1999), or, in case of metal-free stellar populations, in the He  $1640\text{\AA}$ , and  $4686\text{\AA}$  lines out to redshifts  $z \sim 20$  with the mid-infrared instrument (Oh, Haiman & Rees 2001; Tumlinson, Giroux & Shull 2001).

## 7. CONCLUSIONS

The determination by *WMAP* of a high optical depth to Thomson scattering implies that significant reionization took place at redshifts  $z \sim 20$ , and has provided our first glimpse into the earliest structures that exist at these distant epochs. In this paper, we used physically motivated semi-analytical reionization models to quantify the implications of the *WMAP* result. The high value of  $\tau$ , by itself, requires that the earliest light sources have a surprisingly high efficiency  $\epsilon$  of injecting ionizing photons into the IGM. In the running spectral index cosmological model favored by the combination of *WMAP* with other large scale structure data (Spergel et al. 2003),  $\text{H}_2$  molecules are required to form efficiently in halos with virial temperatures  $T_{\text{vir}} < 10^4 \text{ K}$  at high redshifts to produce  $\tau = 0.17$ .

Our most interesting conclusions arise when we require that our models produce (1) a high optical depth  $\tau = 0.17$ , and (2) a percolation epoch at  $z \sim 6-7$ . The latter is required by most interpretations of the rapid evolution in the neutral fraction in the IGM at  $z = 5-6$  (Songaila & Cowie 2002; Becker et al.

2001), and possibly by the high temperature of the IGM inferred from the  $\text{Ly}\alpha$  forest at  $z \sim 4$  (Hui & Haiman 2003). We generically find that no simple model can simultaneously satisfy both of the above requirements. Our results indicate that either  $\text{H}_2$  molecules had to form efficiently at  $z \sim 20$  and allow UV sources in halos with virial temperatures  $T_{\text{vir}} < 10^4 \text{ K}$  to contribute substantially to reionization, or else the ionizing photon production efficiency in halos with  $T_{\text{vir}} > 10^4 \text{ K}$  had to decrease by a factor of  $\gtrsim 30$  between  $z \sim 20$  and  $z \sim 6$ . The first of these two options would have important implications on radiative feedback processes that determine the global  $\text{H}_2$  chemistry. The second option would naturally be explained by the presence of metal-free stars in the earliest halos, which are then replaced by normal stellar populations in larger halos that collapse at later epochs.

The physics of reionization is rich in features that can naturally lead to distinctive ionization histories. These features can arise because of (1) the different types of coolants in halos with virial temperatures above and below  $\sim 10^4 \text{ K}$ , (2) the different response of different halos to radiative feedback on the  $\text{H}_2$  chemistry, and to photoionization feedback on gas infall, and (3) the different properties of metal-free and normal stellar populations. A range of physically motivated reionization histories is allowed by current data. We find that the ionization history in our models generally evolves monotonically with redshift, in difference from “double reionization” that results if the metallicity was increasing uniformly in the IGM, triggering a sharp transition at a fixed redshift from metal-free to “normal” stars. Nevertheless, we find that the evolution of the ionized fractions have sufficiently conspicuous features for Planck to provide tight statistical constraints on reionization model parameters, and to elucidate much of the physics at the end of the Dark Ages. The sources responsible for the high optical depth discovered by *WMAP* should be directly detectable out to  $z \sim 15$  by the *James Webb Space Telescope*.

The *WMAP* result has opened a new window into studies of the first structures at the end of the cosmological dark ages, and has raised the hopes for further interesting findings from all potential probes of the high-redshift universe; including future CMB polarization anisotropy studies, spectroscopic observations of quasars and  $\text{Ly}\alpha$  emitting galaxies at  $z > 6$ , radio probes of the redshifted 21 cm line of neutral hydrogen, as well as direct detections of the sources of reionization and their end-products as supernovae and gamma ray bursts.

We thank Manoj Kaplinghat, Lloyd Knox, and David Spergel for stimulating discussions. GPH is supported by the W.M. Keck foundation. We thank Uros Seljak and Matias Zaldarriaga for the use of their CMBFast code.

## REFERENCES

- Abel, T., Bryan, G. L., & Norman, M. L. 2000, *ApJ*, 540, 39
- Abel, T., Bryan, G. L., & Norman, M. L. 2002, *Science*, 295, 93
- Abel, T., & Haiman, Z. 2001, in “Molecular hydrogen in space”, Cambridge contemporary astrophysics, Eds. F. Combes, and G. Pineau des Forêts, Cambridge University Press: Cambridge, UK, p. 237
- Barkana, R., & Loeb, A. 1999, *ApJ*, 523, 54
- Barkana, R., & Loeb, A. 2001, *Physics Reports*, 349, 125
- Becker, R. H. et al. 2001, *AJ*, 122, 2850–2857.
- Bennett, C. L., et al. 2003, *ApJ*, submitted, astro-ph/0302207
- Bromm, V., Coppi, P. S., & Larson, R. B. 1999, *ApJ*, 527, 5
- Bromm, V., Coppi, P. S., & Larson, R. B. 2002, *ApJ*, 564, 23
- Bromm, V., Ferrara, A., Coppi, P. S., & Larson, R. B. 2001, *MNRAS*, 328, 969

- Bromm, V., Kudritzki, R. P., & Loeb, A. 2001, *ApJ*, 552, 464  
 Bromm, V., & Loeb, A. 2002, *ApJ*, submitted, astro-ph/0212400  
 Chiu, W. A., & Ostriker, J. P. 2000, *ApJ*, 534, 507  
 Ciardi, B., Ferrara, A., & Abel, T. 2000, *ApJ*, 533, 594  
 Cen, R. 2003, *ApJ*, submitted, astro-ph/0210473.  
 Cen, R. and McDonald, P. 2002, *ApJ*, 570, 457–462.  
 Dove, J. B., Shull, J. M., & Ferrara, A. 2000, *ApJ*, 531, 846  
 Eisenstein, D. J., & Hu, W. 1999, *ApJ*, 511, 5  
 Efstathiou, G. 1992, *MNRAS*, 256, 43  
 Fan, X., et al. 2000, *AJ*, 120, 1167  
 Fan, X., et al. 2003, *AJ*, in press, astro-ph/0301135  
 Fan, X., Narayanan, V. K., Strauss, M. A., White, R. L., Becker, R. H., Pentericci, L., and Rix, H. 2002, *AJ*, 123, 1247–1257.  
 Ferrara, A. 1998, *ApJ*, 499, L17  
 Fukugita, M., Hogan, C. J., & Peebles, P. J. E. 1998, *ApJ*, 503, 518  
 Glover, S. C. O., & Brandt, P. W. J. L. 2003, *MNRAS*, in press, astro-ph/0205308  
 Gnedin, N. Y. 2001, *MNRAS*, submitted, astro-ph/0110290  
 Gnedin, N. Y., & Ostriker, J. P. 1997, *ApJ*, 486, 581  
 Gnedin, N. Y., & Shandarin, S. F. 2002, *MNRAS*, 337, 1435  
 Gunn, J. E., & Peterson, B. A., 1965, *ApJ*, 142, 1633  
 Haiman, Z. 2003, *Carnegie Observatories Astrophysics Series, Vol. 1: Coevolution of Black Holes and Galaxies*, ed. L. C. Ho (Cambridge: Cambridge Univ. Press), submitted  
 Haiman, Z., Abel, T., & Madau, P. 2001, *ApJ*, 551, 599  
 Haiman, Z., Abel, T., & Rees, M. J. 2000, *ApJ*, 534, 11  
 Haiman, Z., & Loeb, A. 1997, *ApJ*, 483, 21  
 Haiman, Z., & Loeb, A. 1998, *ApJ*, 503, 505  
 Haiman, Z., & Knox, L. 1999, in “Microwave Foregrounds”, eds. A. de Oliveira-Costa & M. Tegmark (San Francisco: ASP), p. 227  
 Haiman, Z., Rees, M. J., & Loeb, A. 1997, *ApJ*, 476, 458 [erratum: 1997, *ApJ*, 484, 985]  
 Haiman, Z., Thoul, A. A., & Loeb, A. 1996, *ApJ*, 464, 523  
 Holder, G. P., Haiman, Z., Kaplinghat, M., & Knox, L. 2003, *ApJL*, submitted, astro-ph/0302404 (paper II)  
 Hui, L., & Gnedin, N. Y. 1997, *MNRAS*, 292, 27  
 Hui, L., & Haiman, Z. 2003, to be submitted to *ApJ*  
 Jenkins, A., Frenk, C. S., White, S. D. M., Colberg, J. M., Cole, S., Evrard, A. E., Couchman, H. M. P., and Yoshida, N. 2001, *MNRAS*, 321, 372.  
 Kaplinghat, M., Chu, M., Haiman, Z., Holder, G. P., Knox, L., and Skordis, C. 2003, *ApJ*, 583, 24–32.  
 Kogut, A. 2003, *ApJ*, submitted, astro-ph/0302213  
 Leitherer, C., Schaerer, D., Goldader, J. D., Delgado, R. M. G., Robert, C., Kune, D. F., de Mello, D. F., Devost, D., Heckman, T. M. 1999, *ApJS*, 123, 3; electronic data are available at <http://www.stsci.edu/science/starburst99/>  
 Lidz, A., Hui, L., Zaldarriaga, M., & Scoccamarro, R. 2002, *ApJ*, 579, 491  
 Loeb, A. and Barkana, R. 2001, *ARA&A*, 39, 19–66.  
 Machacek, M. E., Bryan, G. L., & Abel, T. 2001, *ApJ*, 548, 509  
 Machacek, M. E., Bryan, G. L., & Abel, T. 2003, *MNRAS*, 338, 273  
 Madau, P., Haardt, F., & Rees, M. J. 1999, *ApJ*, 514, 648  
 MacLow, M.-M., & Ferrara, A. 1999, *ApJ*, 513, 142  
 Miralda-Escudé, J., Haehnelt, M., & Rees, M. J. 2000 *ApJ*, 530, 1  
 Miralda-Escudé, J. 2001, in “The Physics of Galaxy Formation”, ASP Conference Proceedings, Vol. 222, eds. M. Umemura and H. Susa. (San Francisco: ASP), p.181  
 Navarro, J. F., & Steinmetz, M. 1997, *ApJ*, 478, 13  
 Oh, S. P. 1999, *ApJ*, 527, 16  
 Oh, S. P., Haiman, Z., & Rees 2001, *ApJ*, 553, 73  
 Omukai, K., & Nishi, R. 1999, *ApJ*, 518, 64  
 Pentericci, L., et al. 2002, *AJ*, 123, 2151  
 Razoumov, A. O., Norman, M. L., Abel, T., & Scott, D. 2002, *ApJ*, 572, 695  
 Ricotti, M., Gnedin, N. Y., & Shull, J. M. 2002, *ApJ*, 575, 49  
 Seljak, U. and Zaldarriaga, M. 1996, *ApJ*, 469, 437  
 Schaerer, D. 2002, *A&A*, 382, 28  
 Shapiro, P., & Giroux, M.L. 1987, *ApJ*, 321, L107  
 Shapiro, P. R., Giroux, M. L., & Babul, A. 1994, *ApJ*, 427, 25  
 Shapiro, P. R., Raga, A. C., & Mellema, G. 1998, in *Molecular Hydrogen in the Early Universe*, *Memorie Della Societa Astronomica Italiana*, Vol. 69, ed. E. Corbelli, D. Galli, and F. Palla (Florence: Soc. Ast. Italiana), p. 463  
 Songaila, A., & Cowie, L. L. 2002, *AJ*, 123, 2183  
 Spergel, D. N. et al. 2003, *ApJ*, submitted, astro-ph/0302209  
 Steidel, C. C., Pettini, M., & Adelberger, K. L. 2001, 546, 665  
 Tegmark, M., Silk, J., & Blanchard 1994, *ApJ*, 420, 484  
 Tegmark, M., Silk, J., Rees, M. J., Blanchard, A., Abel, T., & Palla, F. 1997, *ApJ*, 474, 1  
 Tumlinson, J., Giroux, M. L., & Shull, J. M. 2001, *ApJ*, 551, 1  
 Tumlinson, J., & Shull, J. M. 2000, *ApJ*, 528, 65  
 Thoul, A. A., & Weinberg, D. H. 1995, *ApJ*, 442, 480  
 Valageas, P., & Silk, J. 1999, *A & A*, 347, 1  
 Venkatesan, A. 2000, *ApJ*, 537, 55  
 Venkatesan, A. 2002, *ApJ*, 572, 15  
 Wood, K. & Loeb, A. 1999, *ApJ*, 545, 86  
 Wyithe, S. and Loeb, A. 2003, *ApJ*, in press, astro-ph/0209056.  
 Zaldarriaga, M. 1997, *Phys. Rev. D*, 55, 1822

TABLE 1

COLLAPSE REDSHIFTS AND MASSES OF 1, 2 AND  $3\sigma$  DARK MATTER HALOS WITH VIRIAL TEMPERATURES OF  $T_{\text{vir}} = 100$  AND  $10^4\text{K}$ , REFLECTING THE MINIMUM GAS TEMPERATURES REQUIRED FOR COOLING BY  $\text{H}_2$  AND NEUTRAL ATOMIC H, RESPECTIVELY.

$T_{\text{vir}}(\text{K})$	$\nu$	$z_{\text{coll}}$	$M_{\text{halo}}(M_{\odot})$
100	1	7	$2 \times 10^7$
	2	16	$5 \times 10^4$
	3	26	$3 \times 10^4$
$10^4$	1	3.5	$4 \times 10^8$
	2	9	$1 \times 10^8$
	3	15	$6 \times 10^7$

TABLE 2

CONSTRAINTS ( $\Delta\bar{\chi}^2$ ) FROM FUTURE CMB POLARIZATION EXPERIMENTS ON THREE MODELS WITH THE SAME  $\tau = 0.17$ .

Model pair	2-yr <i>WMAP</i>	Planck	Cosmic variance
AB	0.2	9	25
AC	0.1	2.6	18
BC	0.3	13	34
A vs one-step	0.3	16	60